ICCP Commission II

Igneous intrusions in coal seams and shales Working Group

Conveners:

Sandra Rodrigues

Jolanta Kus

Magdalena Misz-Kennan

Susan Rimmer

June 2025

2024/2025 Round Robin Exercise

The Igneous Intrusions in Coal Seams and Shales Working Group was created in 2022 during the 73rd ICCP meeting in India. One of the main objectives of this WG is to investigate the petrographic changes in coals, dispersed organics, and mineral matter induced by contact metamorphism. Associated with the petrographic work are other analyses, including, where possible, Raman spectroscopy, micro-FTIR, Rock-Eval, GC-MS, biomarkers, SEM/EDS, XRD, XRF or ash, volatile matter, and moisture contents. This set of analyses will help to understand the chemical and structural transformations undergone by both organics and mineral matter affected by the temperature and pressure fields associated with igneous bodies. This WG will also look at the impact of the emplacement of the igneous intrusions on neighbouring strata, which can include deformation on a megascopic scale, such as folding and fracturing, columnar jointing, and other megascopic alterations.

The objective of the first Round Robin (RR) exercise of this WG is, primarily, to assess the setup of the exercise, including: i) type of images, e.g., non-polarised and polarised reflected white light, the addition of a lambda plate, fluorescence mode; ii) reflectance information; e.g., VRr%, VRmax% and VRmin%, iii) the use of squares and pointers to indicate the materials that are being evaluated; and iv) appropriate classification.

There are several factors that may affect the organic matter in coal or shales, including the coal rank/ thermal maturity of the organic material at the time of the intrusion, proximity to the igneous intrusion, temperature, shape, type and size of the igneous intrusion, pressure, lithology of the surrounding rocks, among others. Typical optical changes caused by an intrusion include an increase in the vitrinite reflectance, decreased ability to identify liptinite macerals, development of devolatilization pores, formation of coke textures (including petroleum coke in shales), pyrolytic carbon, and graphite, the appearance of fractures, microbrecciation, and folding. The current exercise will test the hierarchy of the classification scheme.

Sample Information and analyses

The background Suluova coal (sample number 2309295) was collected from the Yeni Celtek coal mine, Amasya-Suluova Basin by Ali Ihsan Karayigit (Hacettepe University, Turkey). Measurements of the mean random reflectance of ulminite (mainly eu-ulminite A) vary between 0.46 and 0.60% (0.53% average) (Karayigit et al., 1996). The Early Eocene coke (sample number 2309296) was taken from a borehole at 229.45-229.60 m located between two magmatic intrusions, that is, 10.55 m depth from the upper magmatic intrusion and 105.95 m above the lower magmatic intrusion.

Chemical, Rock-Eval analyses (Table 1), FTIR, and XRD were conducted on the original coal (sample number: 2309295) and the coke (2309296). The total carbon (TC) and total sulfur (TS) contents were measured using a LECO CS 744 Carbon-Sulfur Analyzer after combustion at around 2000°C in an oxygen stream. For organic carbon (C_{org}), samples were decarbonated with 10% HCl at 80°C before analysis to remove carbonate carbon. Rock-Eval Pyrolysis was carried out according to the classical standard method (Espitalié et al., 1977) using a Rock-Eval 6 instrument. The measurement of pyrolysis products was performed using a flame ionization detector (FID), while the released carbon dioxide (CO_2) was determined with an infrared detection cell. The temperature program starts with an isothermal step of 3 minutes at 300°C, followed by a heating phase up to 650°C at a heating rate of 25°C/min.

Table 1. Geochemical data of the samples.

Samples	2309295	2309296	2309297
TC%	68.8	85.5	56.5
Corg%	60.6	83.8	56
TS%	1.25	0.13	0.26
S1 mg/g	1.77	0.29	0.93
S2 mg/g	219.22	5.93	4.17
S3 mg/g	3.77	0.65	1.86
Tmax%	406	508	353

TC – Total carbon; Corg – organic carbon; TS – total sulphur; S1 – free and adsorbed hydrocarbons released during isothermal phase; S2 – generated hydrocarbons from the cracking of kerogen during pyrolysis; S3 – CO_2 released during pyrolysis; Tmax – temperature at which the maximum hydrocarbons released in S2 occurs.

X-ray diffraction (XRD) analyses were also carried out and showed that quartz and pyrite are the main mineralogical phases in the coal, whereas in the natural coke, quartz together with carbonate phases, such as calcite and ankerite, are the main mineral constituents. An amorphous phase is present in both samples which corresponds to the organic matter.

For image acquisition and reflectance measurements, a Leica DMRX incident light microscope was used that was equipped with an MPV Compact 2 microphotometer photomultiplier tube (PMT), halogen lamp (12 V, 100 W), HBO® Lamp (103 W/2, 12 V), and Leica Oil P 50×/0.85 oil-immersion objective; Leica Type F immersion oil ne = 1.518 (23 C). A Leica digital fluorescence camera DC 310F at 1.300 × 1030 pixels and Image Access Premium 09 software were used for generation of photomicrographs. Photomicrographs were captured under non-

polarised and polarised incident white light, and some images were collected with a lambda plate (1λ) insertion.

Instructions for the participants

In the first level, the participants are required to differentiate between organic matter/carbon materials and mineral matter (although an empty space can also be indicated). **If the organic matter/carbon materials option is selected, the participant needs to characterize these materials regarding their alteration state (information relative to the original coal is available to the participants), optical anisotropy (reflectance values and photomicrographs with polarised light and lambda plate aid in the identification of anisotropy), and occurrence of newly formed particles (which implies the complete transformation of the organic material and/or precipitation of carbon material). If in the selected area, the participants may need to identify the microstructure present.** For the current exercise, the mineral matter section is very simplified, however, the conveners will expand this section in the upcoming exercises.

The current exercise is comprised of 22 images of high volatile and medium volatile bituminous coals from Turkey heat affected by igneous intrusions. The conveners are grateful to Professor Ali Ihsan Karayigit (Hacettepe University, Turkey) for the samples. The participants will receive a PowerPoint presentation with those images, an Excel file in which the participant will fill in answers, and a letter stating the objectives of the WG and RR as well as the description of the properties and microstructures considered in this RR. Note that, with time and access to more thermally altered organic materials, this classification scheme will incorporate additional terms.

Feedback on the exercise is most appreciated. Only with feedback of the participants it is possible to improve the upcoming exercises.

It is anticipated that the participants of the Igneous Intrusions in Coal Seams and Shales WG Exercise 2024/2025 will submit the results electronically by **July 30, 2025**, in the form of established exercise sheets to Sandra Rodrigues (sandra23rodrigues@gmail.com).

Classification Scheme for thermally affected coals by igneous intrusions

A. Type of material

Organic/carbon material vs minerals (<u>Choose one option</u>)

This section allows differentiation between organic components (macerals) either from coal or dispersed organic matter in sediments and carbon materials from minerals (Fig. 1).

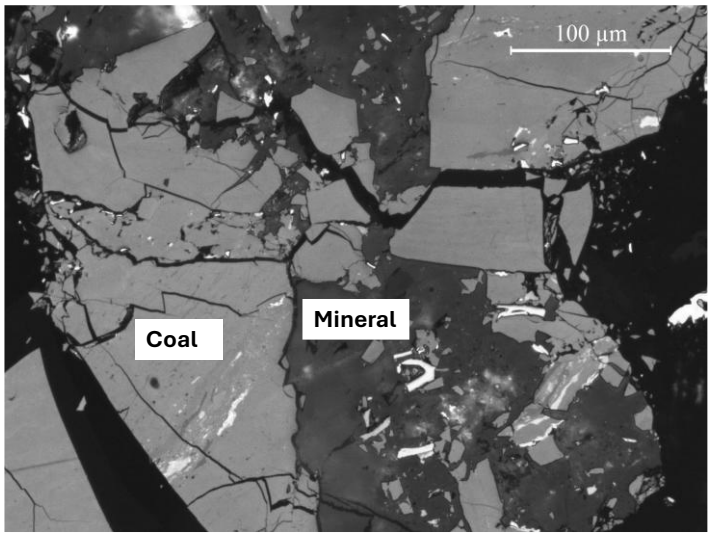

Fig. 1. Coal particle with fracture filled with mineral matter, possibly carbonates from Bowen Basin, Australia (photomicrograph from S. Rodrigues). Image taken in non-polarised white light.

B. Characterisation of the organic/carbon materials

1. Optical anisotropy (Choose one option)

1.1. Isotropic: no observable optical anisotropy as observed in the images in polarised light and ¼ lambda plate (magenta colour) (Fig. 2a, b).

1.2. Anisotropic: optical anisotropy observable by the change in the colour with polarised light and ¼ lambda plate (from yellow, pink, blue interference colours) (Fig. 2c, d).

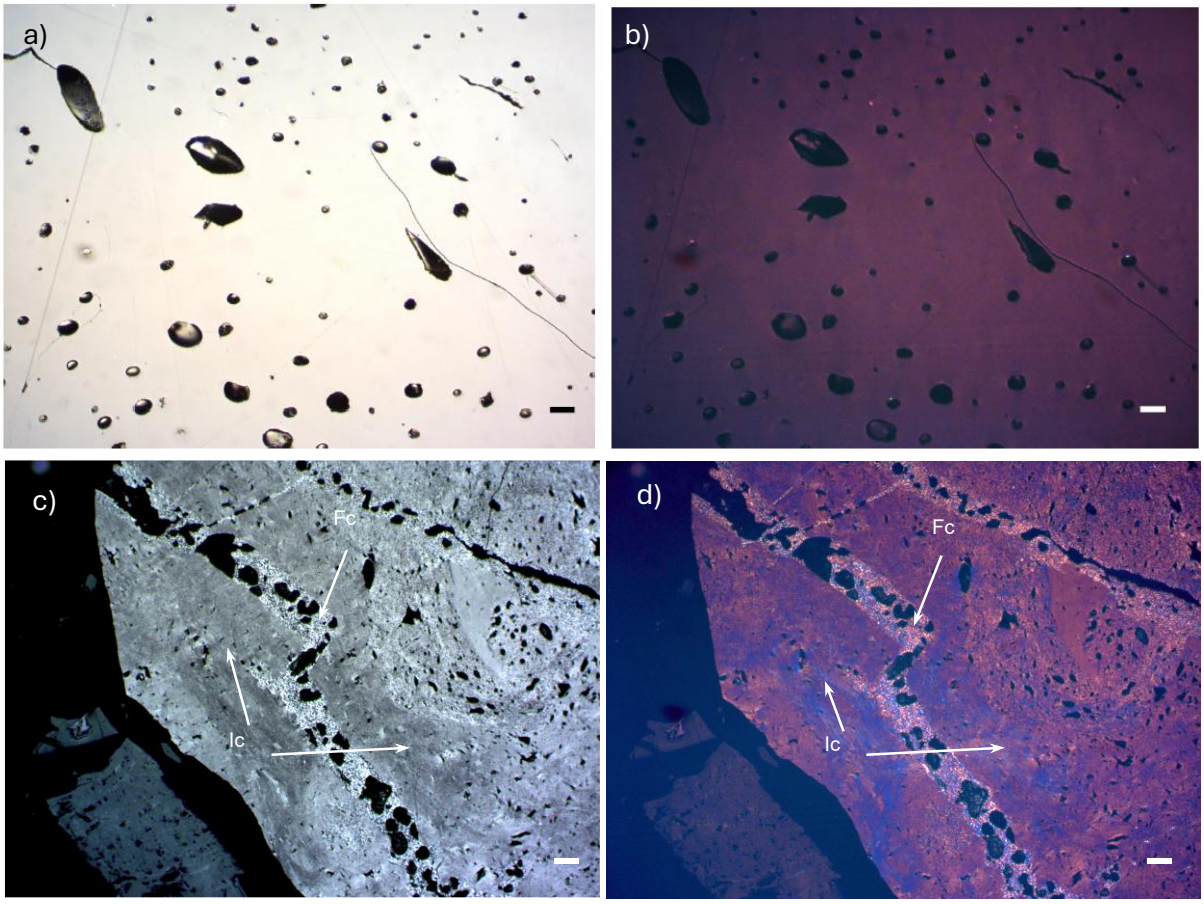

Fig. 2. a) and b) Example of isotropic coke (Rr=2.75%) showing devolatilization vacuoles and minor fractures observed in sample from the Herrin (No. 6) coal seam (background coal 0.55-0.57% Rr) in the Illinois Basin, USA. c) and d) Example of anisotropic coke (Rr=5.88%) from Piceance Basin, Colorado, USA, background coal Rr=0.75%. Photomicrographs from S. Rimmer. Image a) non polarized light; c) partially crossed polarizers; b and d) crossed polarizers and 1/4 λ plate). Scale bar: 20 μm.

2. Degree of Thermal Alteration (<u>Choose one option</u>)

2.1. Non-altered macerals: background coal (Fig. 3a).

2.2. Altered macerals: the reflectance is higher than the reflectance of the background coal (i.e., above the non-altered coal) (Fig. 3b). Optical features (besides changes in the reflectance) that are indicative of thermal alteration might be present, for example the presence of natural coke (Fig. 3c).

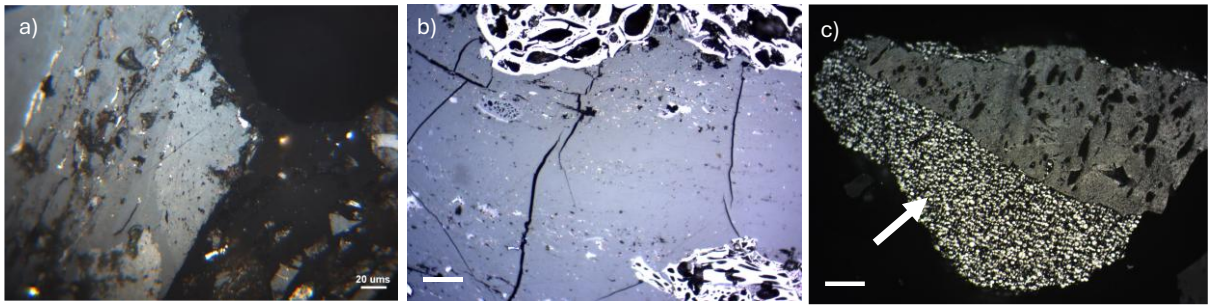

Fig. 3. a) non-altered coal particle (Rr= 0.55%) from Illinois Basin (Presswood et al., 2016); b) Altered coal particles (Rr= 1.28%) from Piceance Basin, Colorado, USA (background coal Rr=0.75%) (photomicrograph from S. Rimmer); c) Natural coke particle from Piceance Basin, Colorado, USA photomicrograph from S. Rimmer). a) and b) non-polarised white reflected light; c) partially crossed polarizers. Scale bar: 20 µm.

3. Newly formed particles (Choose one option)

3.1. Natural Coke (**isotropic, incipient, circular, lenticular, ribbon).** Natural coke is coal altered by the relatively local elevated heat flow caused by an intrusive body (Kwiecińska and Petersen, 2004). Molten and resolidified material (particularly from vitrinite and liptinite macerals) which will no longer be recognisable as macerals. However, the banding (e.g., vitrinite) or morphology (e.g., liptinite) can sometimes be preserved. It may present variable optical anisotropy (isotropic, Fig. 4a, b, and anisotropic) and variable mosaic microtextures such as incipient (Fig. 4c, d), circular (Fig. 4 c, d, Fig. 5 and Fig. 6a), lenticular, and ribbon (Fig. 6b). The circular texture seems to be the most prevalent mosaic texture reported in the literature; however, that is more a function of the original rank of the coal at the time of magma intrusion.

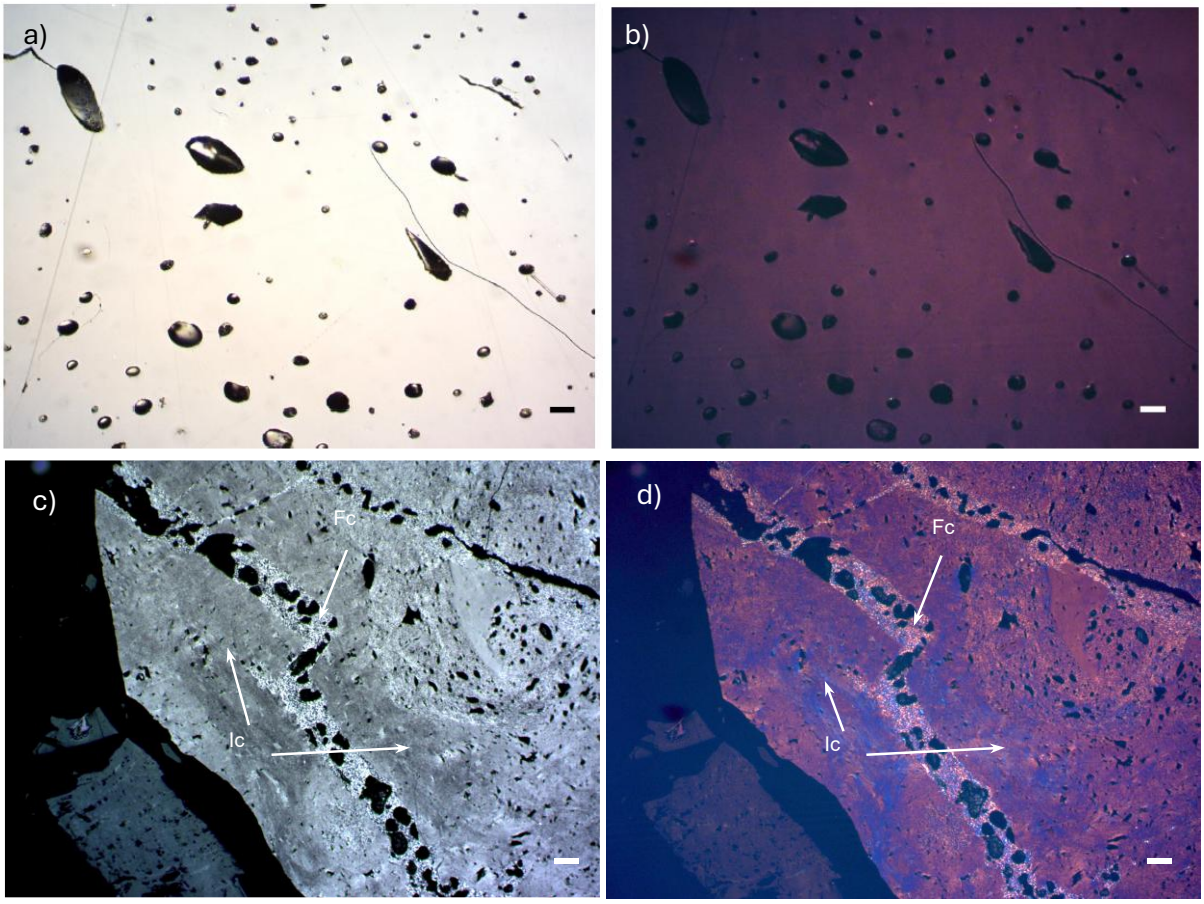

Fig. 4. a) and b) Example of isotropic coke (Rr=2.75%) showing devolatilization vacuoles and minor fractures observed in sample from the Herrin (No. 6) coal seam (background coal 0.55-0.57% Rr) in the Illinois Basin, USA.c) and d) Example of incipient coke (Ic) and fracture fill with fine-grained circular mosaic (Fc) from Piceance Basin, Colorado, USA Background coal Rr = 0.75% (photomicrographs from S. Rimmer et al., in prep). a) non polarized light; c) partially crossed polarizers; b and d) crossed polarizers and 1/4 l plate). Scale bar: 20 µm.

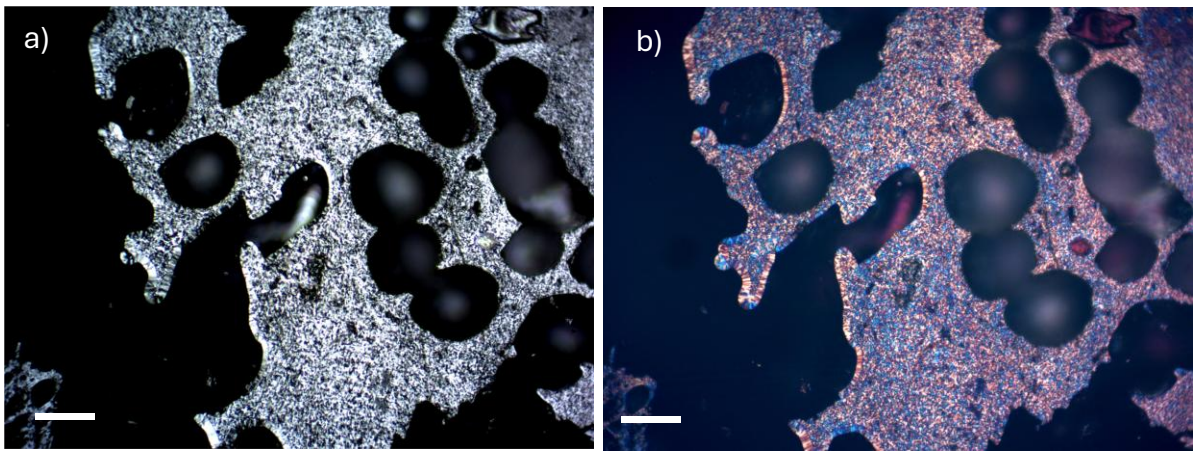

Fig. 5. Example fine circular coke from Piceance Basin, Colorado, USA. Background R_r = 0.75%. Rr – 5.88% (photomicrographs from S. Rimmer). a) partially crossed polarizers; d) crossed polarizers and 1/4 λ plate). Scale bar: 20 µm.

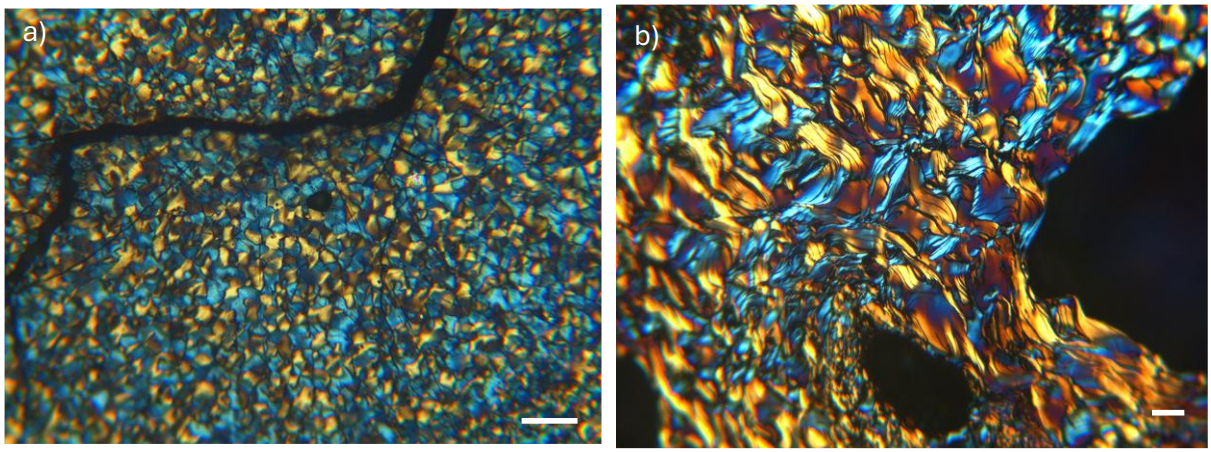

Fig. 6. Examples of a) medium- to coarse-grained circular mosaic in coked coal and b) medium-grained ribbon mosaic with some pore development (PR4) developed in coked bitumen from Purgatoire River, Colorado, USA. Background coal Rmax ~ 1.0% (Rimmer et al., 2015). Crossed polarizers and antiflex objective (incorporates a ¼ λ plate). Scale bar = 20 μm.

3.2. Pyrolytic Carbon (PC): This is a type of carbon deposit formed by the chemical cracking of volatiles generated by thermally altered coals during igneous intrusions (Kwiecińska and Pusz, 2016). It usually occurs as small spheres with a distinctive cone structure and highly anisotropic with 1 to 10 μm diameter (Goodarzi, 1985; Kwiecińska and Pusz, 2016), although other microstructures can also occur such as lamellar, substrate-nucleated, spherulitic, and isotropic (Fig. 7). It can occur on the border of the maceral particles or inside fractures.

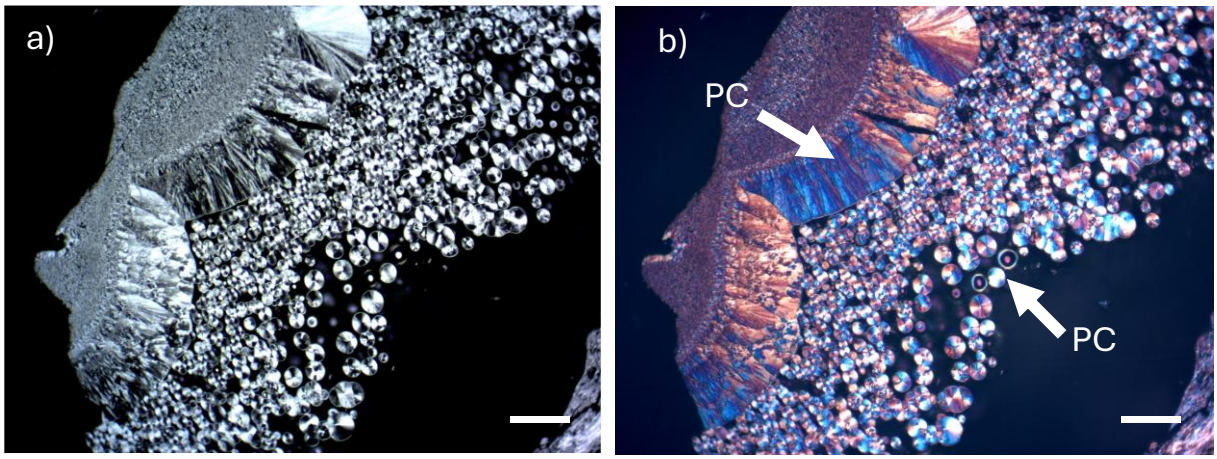

Fig. 7. Example of pyrolytic carbon, PC, Piceance Basin, Colorado, USA Background R_r = 0.75%. (photomicrograph from S. Rimmer). a) partially crossed polarizers; d) crossed polarizers and 1/4 λ plate). Scale bar: 20 μm.

3.3. Graphite-like particles (microcrystalline graphite, flakes, needles): These result from the solid transformation of coal (contrary to coke), particularly in the coal of anthracite rank. Microcrystalline graphite has a granular texture (Fig. 8), which can be

confused with natural coke; however, it usually occurs with other graphitic structures such as needles or flakes. Needle-shaped graphite has a very fine (fiber-like) appearance (Fig. 8c), whereas flakes (Fig. 8d) can have variable thickness (Li et al., 2019). Scale bar: 20 μm.

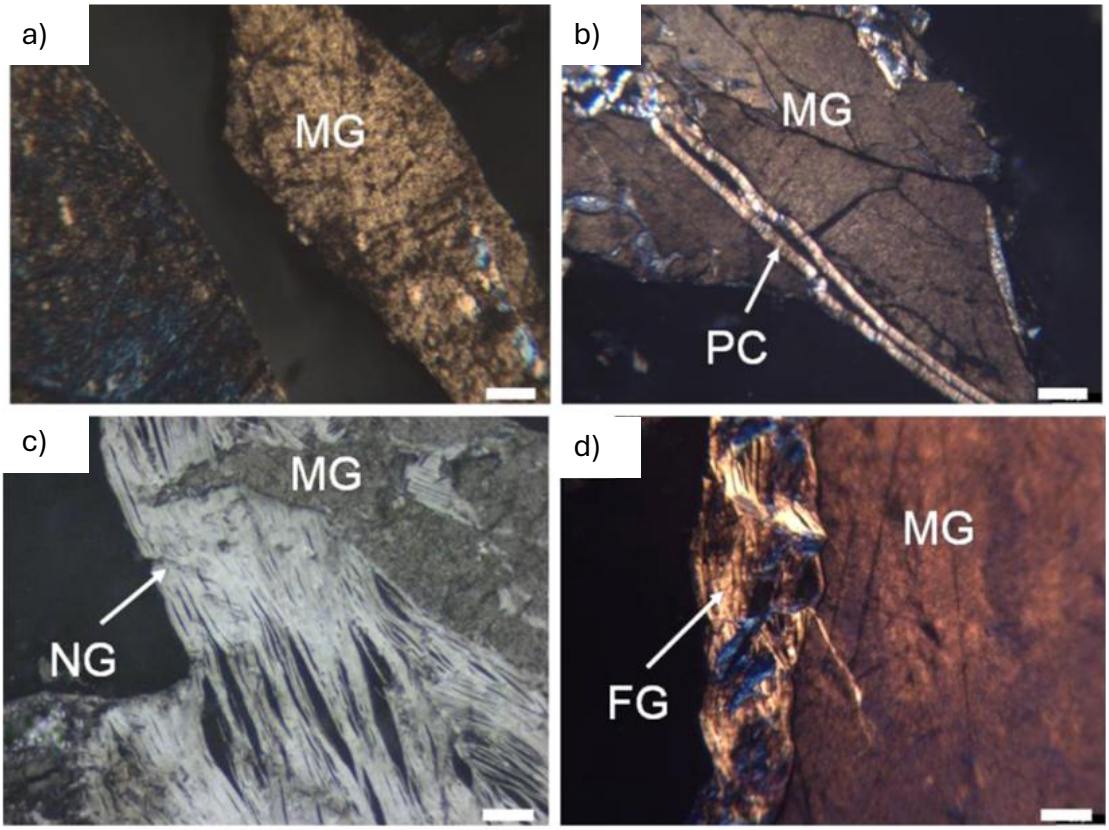

Fig. 8. Microscopic forms of graphitic structures. MG – microcrystalline graphite; NG – needle graphite; FG – flake graphite; PC – pyrolytic carbon. Images from Li et al. (2019). Images taken under white light, 40× antiflex objective and oil immersion, crossed polarizers were used (except for c). Scale bar: 20 μm.

3.4. Coked bitumen: results from the thermal alteration of bitumen that was generated prior to or in the early stages of the igneous event. It can be anisotropic presenting ribbon coke structures similar to petroleum coke (Fig. 9) (Rimmer et al., 2015) but it can also develop highly anisotropic parallel laminae (Fig. 10a) and, in other cases, fine-grained circular mosaic with bands of anisotropic coke and pyrolytic carbon (Fig. 10b).

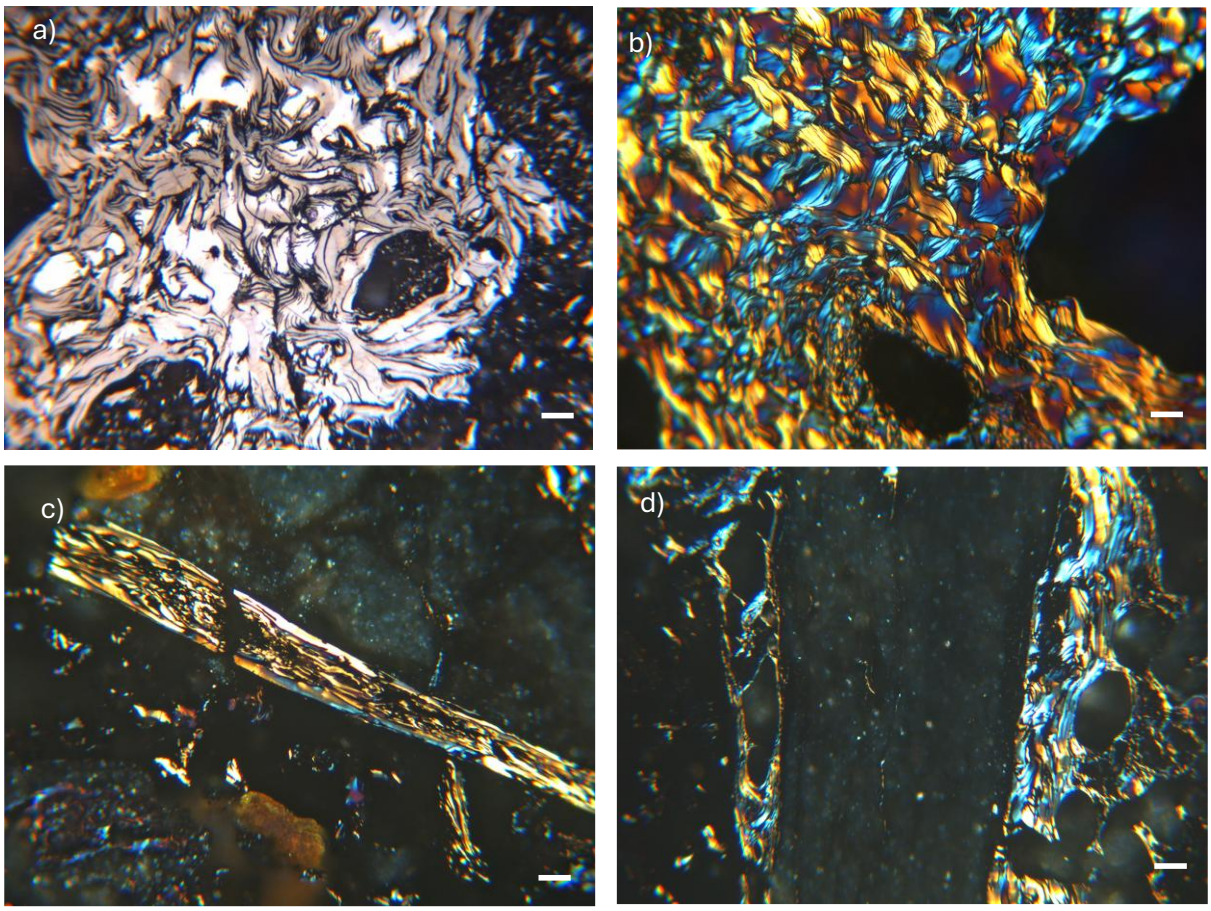

Fig. 9. Examples of coked bitumen from the Purgatoire River Valley, Raton Basin (Rimmer et al., 2015). a) coked bitumen in coke "fingers" showing medium-grained ribbon mosaic texture (PR4) (non-polarized light); b) medium-grained ribbon mosaic with some pore development (PR4); c) and d) porous coke in fractures adjacent to shale fragment (PR5); b) to c) the images were taken using crossed polarizers using an antiflex objective (which incorporates a ¼ λ plate). Scale bar = 20 μm.

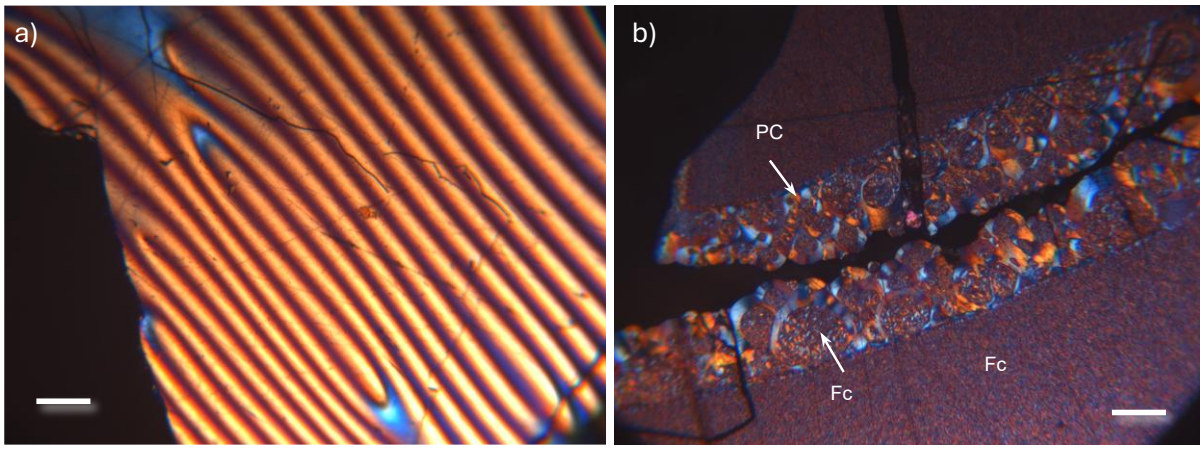

Fig. 10. Examples of coked bitumen from Nanisivik Mississippi Valley-type deposit, Baffin Island, Canada (Gize and Rimmer, 1983 samples). a) Highly developed anisotropy in coked bitumen with parallel laminae; b) Fine-grained circular mosaic (Fc) with coarser, arcuate bands of anisotropic coke

and pyrolytic carbon (PC). Images taken using crossed nichols using antiflex objective (which incorporates a ¼ l plate. Scale bar = 20 μm.

C. Characterisation of microstructures

(Choose one option)

Devolatilization pores are small openings usually with a round or oval shape, that form in the coal matrix during the process of heating and volatile release (Taylor et al., 1998) (Fig. 11). It does not refer to cellular structure. For example, the fusinite cell structure should not be classified as porous, unless the cell walls themselves present porosity.

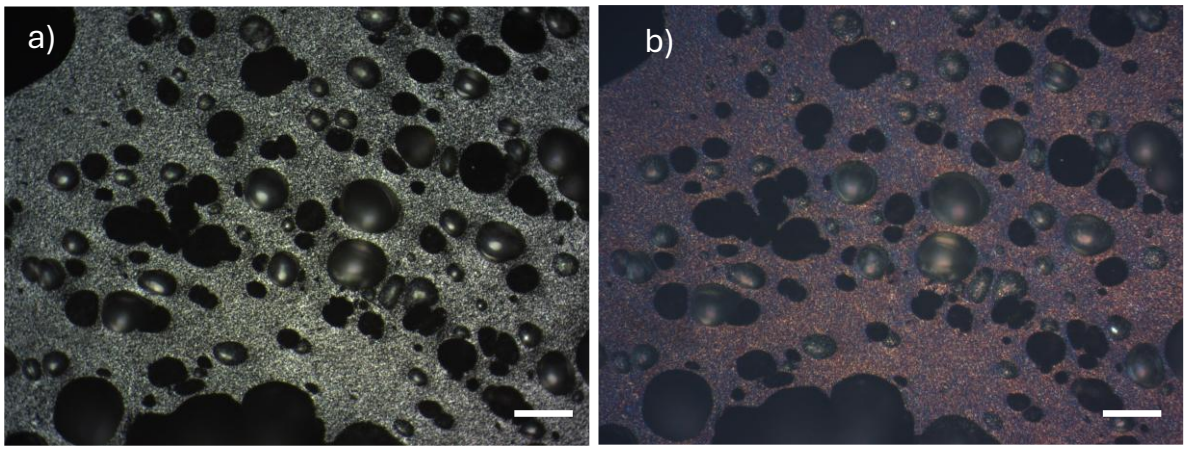

Fig. 11. Example of devolatilization pores from the Piceance Basin, Colorado, USA Background R_r = 0.75% (photomicrographs from S. Rimmer). a) partially crossed polarizers; b) crossed polarizers and 1/4 λ plate. Scale bar: 20 μm.

Microfractures: Microfractures may cut across the different coal or coke layers, although they can also be parallel to the banding (Fig. 12). They may also present some displacement of the coal layers but without total rearrangement of the coal particles (see microbrecciation). The fractures may or may not be filled with minerals. (In the image below the coal is fractured but not brecciated).

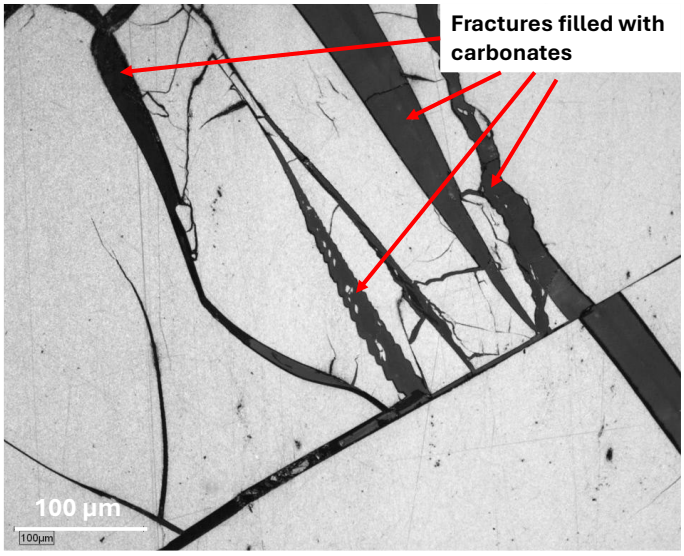

Fig. 12. Example of fractures in incipient coke (Rr=2.38%) from Moatize Basin, Mozambique. Background coal Rr= 1.27%. Photomicrographs taken reflected white light, 20x air objective (photomicrographs from S. Rodrigues).

Coal/coke breccia: angular coal or coke fragments of different sizes that usually present different orientations (Fig. 13). The fragments can be cemented (cohesive brecciation, Fig. 13a) or not (incohesive brecciation, Fig. 13b) (Passchier and Trouw, 2005). The use of polarised light allows observation of the coal fragments with different orientations, which indicates that brecciation occurred after the thermal event.

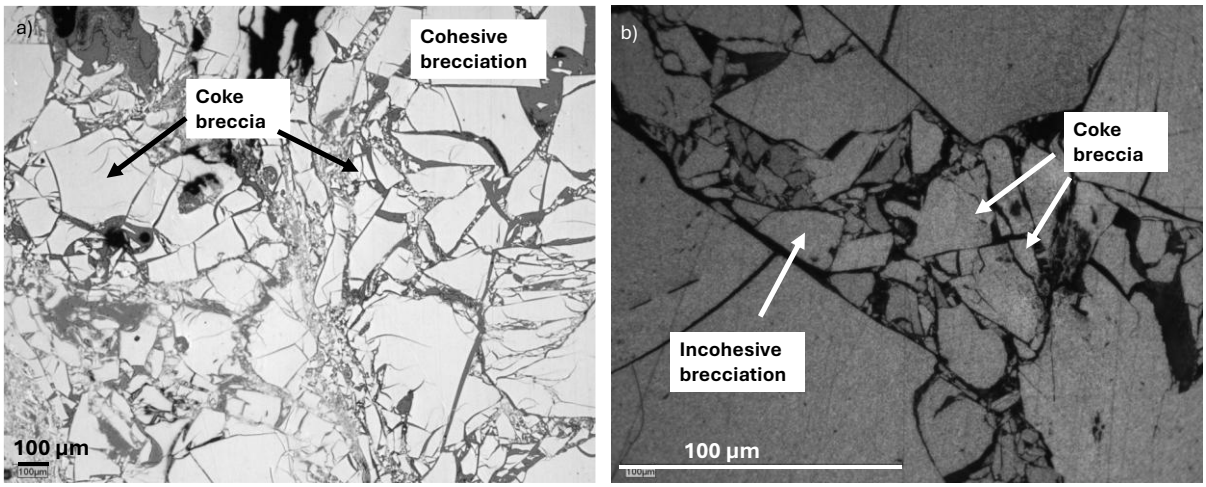

Fig. 13. Example of coke breccia (Rr=2.41%) from Moatize Basin, Mozambique. Background coal Rr = 1.27%. a) reflected white light, 5x air objective; b) reflected polarized white light, 50x oil immersion objective (photomicrographs from S. Rodrigues).

Microfolds: Microfolding occurs within the coal banding or within the molten material as a result of ductile deformation (Fig. 14). The structure of the coal changes shape without breaking.

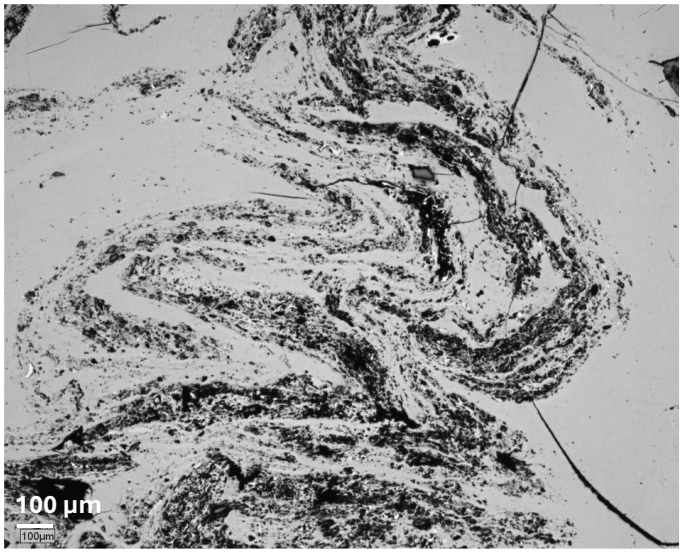

Fig. 14. Example of microfolding (Rr=2.41%) from Moatize Basin, Mozambique. Background coal Rr = 1.27%. Photomicrograph taken in reflected white light, 5x air objective (photomicrograph from S. Rodrigues).

Injection of molten material: Injection of molten materials into fractures that cut across different layers, either other sediments (Fig. 15a) or coal layers (Fig. 15b) but show a difference in the material composition between the injected material and the host. The injected material can be derived from melted coal (Podwysocki and Dutcher, 1971; Rimmer et al., 2025) or tar or bitumen formed either from the coal or organic matter in adjacent layers (Rimmer et al., 2015).

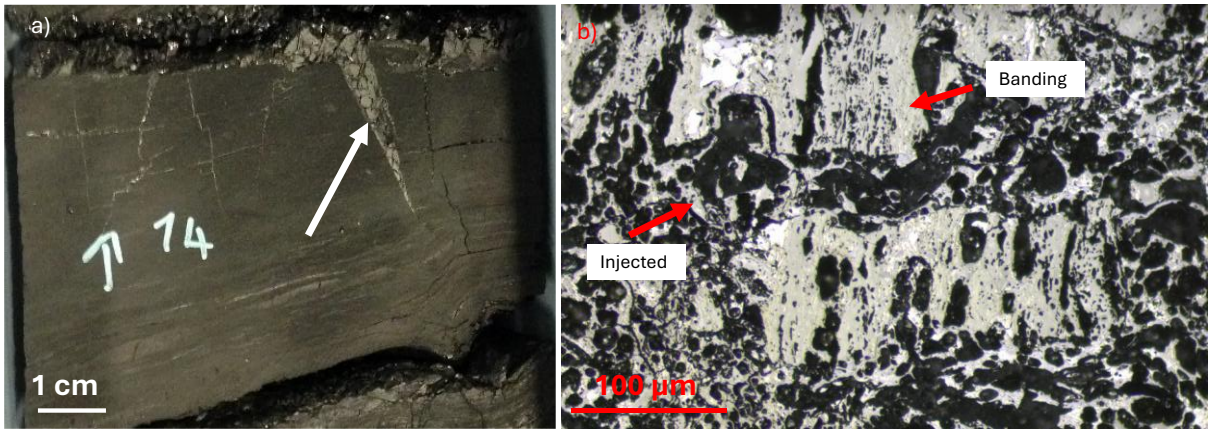

Fig. 15. Examples of injection of molten material. a) piece of core showing injection of molten coal into the carbonaceous mudstone from Moatize Basin, Mozambique. b) molten coal cutting through the coked coal banding (reflected white light with 20x oil immersion objective) from Bowen Basin, Australia. (photomicrographs from S. Rodrigues).

D. Characterisation of mineral matter

Metallic vs non-metallic

Metallic: Mineral has a metallic appearance, for example sulfides such as pyrite (Fig. 16a).

Non-metallic: Mineral has a glassy appearance (for example, quartz), or a crystalline one with internal reflections (for example, carbonates), or a granular or flaky appearance (for example, clays) (Fig. 16b).

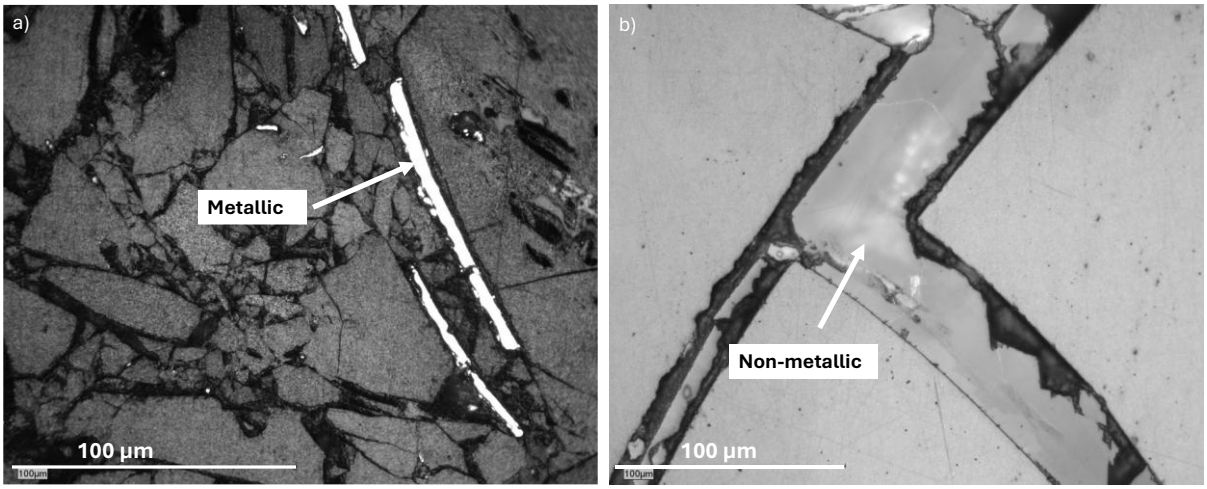

Fig. 16. Examples of mineralisation from the Moatize Basin, Mozambique. Background coal Rr=1.27%. a) metallic mineral (coke Rr= 2.21%), photomicrograph taken with reflected polarized white light, 50x oil immersion objective; b) Non-metallic mineral (coke Rr=2.38%), photomicrograph taken with reflected white light, 20x air objective. Photomicrographs from S. Rodrigues.

Reference list:

ASTM D5061-07. Standard method for microscopical determination of the textural components of metallurgical coke. West Conshohocken, US. 6 pages.

Espitalié, J.L. Laporte, M. Madec, F. Marquis, P. Leplat, J. Paulet, A. Boutefeu, Méthode rapide de caractérisation des roche mères, de leur potentiel pétrolier et de leur degré d'évolution; Revue de l'Institut Français du Pétrole, 32 (1977), 23–42

Gize, A.P., Rimmer, S.M., 1983. Mesophase development in a bitumen from the Nanisivik Mississippi Valley-Type deposits. Year Book 82. Carnegie Inst., Washington, 414–419.

Goodarzi, F., 1985. Characteristics of pyrolytic carbon in Canadian coals. Fuel 64, 1672–1676.

Kwiecińska, B. Pusz, S., 2016. Pyrolytic carbon – Definition, classification and occurrence. International Journal of Coal Geology 163, 1–7.

Kwiecińska, B., Petersen, H.I., 2004. Graphite, semi-graphite, natural coke, and natural char classification – ICCP system. International Journal of Coal Geology 57, 99–116.

Li, K., Rimmer, S.M., Presswood, S.M., Lui, Q., 2020. Raman spectroscopy of intruded coals from the Illinois Basin: Correlation with rank and estimated alteration temperature. International Journal of Coal Geology 219, 103369.

Li, K., Rimmer, S.M., Liu, Q., Zhang, Y., 2019. Micro-Raman spectroscopy of microscopically distinguishable components of naturally graphitized coals from Central Hunan Province, China. Energy & Fuels 33, 1037–1048.

Passchier, C.W., Trouw, R.A.J., 2005. Microtectonics. 2nd revised and enlarged edition. Springer-Verlag, Germany. 372 p.

Podwysocki, M.H., Dutcher, R.R., 1971. Coal dikes that intrude lamprophyre sills; Purgatoire River Valley, Colorado. Economic Geology 66, 267–280.

Presswood, S.M., Rimmer, S.M., Anderson, K.B., Filiberto, J., 2016. Geochemical and petrographic alteration of rapidly heated coals from the Herrin (No. 6) coal seam, Illinois Basin. International Journal of Coal Geology 165, 243–256.

Rimmer, S.M., Yoksoulian, L.E., and Gröcke, D.R., 2025. Contact metamorphism of coals in the southern Piceance Basin, USA: Volatile matter generation, pyrolytic carbon accumulation, and $\delta^{13}C_{org}$ trends. Evolving Earth 3, 100063,

Rimmer, S.M., Crelling, J.C., Yoksoulian, L.E., 2015. An occurrence of coked bitumen, Raton Formation, Purgatoire River Valley, Colorado, U.S.A. International Journal of Coal Geology 141-142, 63–73.

Taylor, G.H., Teichmuller, M., Davius, D., Diessel, C.F.K., Littke, R., Robert, P., 1998. Organic Petrology, Gebruder Borntraeger, Berlin, Stuttgart. 704 p.